Connectivity in the human brain dissociates entropy and complexity of auditory inputs ☆

CrossMark

Samuel A. Nastase [a,c,*], Vittorio Iacovella [a], Ben Davis [a], Uri Hasson [a,b]

[a] Center for Mind/Brain Sciences (CIMeC), The University of Trento, 38123 Mattarello, Italy
[b] Department of Psychology and Cognitive Sciences, The University of Trento, 38122 Trento, Italy
[c] Department of Psychological and Brain Sciences, Dartmouth College, Hanover, NH 03755, USA

ABSTRACT

Complex systems are described according to two central dimensions: (a) the randomness of their output, quantified via entropy; and (b) their complexity, which reflects the organization of a system's generators. Whereas some approaches hold that complexity can be reduced to uncertainty or entropy, an axiom of complexity science is that signals with very high or very low entropy are generated by relatively non-complex systems, while complex systems typically generate outputs with entropy peaking between these two extremes. In understanding their environment, individuals would benefit from coding for both input entropy and complexity; entropy indexes uncertainty and can inform probabilistic coding strategies, whereas complexity reflects a concise and abstract representation of the underlying environmental configuration, which can serve independent purposes, e.g., as a template for generalization and rapid comparisons between environments. Using functional neuroimaging, we demonstrate that, in response to passively processed auditory inputs, functional integration patterns in the human brain track both the entropy and complexity of the auditory signal. Connectivity between several brain regions scaled monotonically with input entropy, suggesting sensitivity to uncertainty, whereas connectivity between other regions tracked entropy in a convex manner consistent with sensitivity to input complexity. These findings suggest that the human brain simultaneously tracks the uncertainty of sensory data and effectively models their environmental generators.

Introduction

Theoretical and experimental work in the fields of psychology and complexity science has arrived at two separate approaches for describing how stimuli may be encoded and what constitutes a complex stimulus (see Shiner et al., 1999). The first aims at explaining to what extent a specific stimulus can be considered "simple" from the perspective of a machine whose goal is to veridically encode and reproduce that stimulus (e.g., Chater and Vitanyi, 2003). For example, the stimulus *ABCDABCD* is quite simple because it can be represented as "repeats *ABCD* twice," whereas *ACDDBADC* is substantially more complex because it requires more memory to encode. Within this framework, simple stimuli are therefore those that contain noticeable patterns; they permit compressed representation, are easy to manipulate and provide a basis for predicting future states. Importantly, from this perspective, "complexity" scales monotonically with stimulus disorder

(entropy), as more disordered inputs are less compressible—that is, increasingly random stimuli require more memory in order to be veridically reproduced.

On the other hand, the second, more recent view (e.g., Crutchfield, 2012) holds that simplicity/complexity depends on how demanding it is to model the underlying system that generated a particular stimulus or signal via the interactions of its states. From this perspective, there is a convex, inverse U-shaped relation between disorder and complexity. This is because highly ordered and highly disordered signals are typically generated by succinct, easily describable systems, whereas more sophisticated, or complex, systems generally convey intermediate levels of entropy.[1] Note that in this latter approach, complexity does not capture how difficult it is to veridically encode or reproduce any specific stimulus or signal, but rather how computationally demanding it is to model the system or source generating that signal. As can be appreciated, the two views described above are independent, and graphs depicting

[1] For instance, *ABCDABCD* can be thought of as generated by a system (e.g., a transition matrix) that transitions between four states deterministically (a simple explanation), while a random stimulus can be characterized by a system where all state transitions are equally likely (a similarly simple explanation).

monotonic vs. convex complexity–entropy relations are the subject of ongoing theoretical discussion (e.g., Feldman et al., 2008).

There has been substantial theoretical and behavioral support, as well as some validation from neuroimaging studies, for the importance of entropy in sensory and cognitive processing, as detailed below. However, there is as yet little evidence that the human brain codes for environmental inputs in a way consistent with the second view arguing for a convex relation. The current study was motivated by the hypothesis that, from a cognitive perspective, these two properties are complementary. In the following, we argue that the human brain tracks both disorder (the degrees of freedom in sensory data) and complexity (quantified, e.g., by the degrees of freedom or minimum message length specifying a model of those data; Spiegelhalter et al., 2002; Wallace, 2005). This sort of dual encoding model suggests that neural sensitivity to uncertainty may vary both linearly and convexly in response to stimuli of increasing entropy. We then present a functional MRI study addressing this hypothesis.

Sensitivity to entropy is crucial for compression (Barlow, 1961; Borst and Theunissen, 1999; Brady et al., 2009; Buiatti et al., 2009; Olshausen and Field, 1996), prediction (Kiebel et al., 2008) and guiding adaptive behavior (Ashby, 1947; Friston, 2010). Prior neuroimaging studies have documented neural systems whose activity monotonically tracks the degree of uncertainty in sensory inputs, particularly in lateral temporal cortex (Bischoff-Grethe et al., 2000; Tobia et al., 2012), the anterior cingulate (Harrison et al., 2006, 2011), and the hippocampus (Strange et al., 2005), even in the context of passive listening (Tobia et al., 2012; Tremblay et al., 2012) or passive viewing (Nastase et al., 2014). Behavioral work has shown that humans track parameters related to entropy, such as token frequency (Shannon entropy; e.g., Berlyne, 1957; Vitz, 1966, 1964), transition constraints (Markov entropy; e.g., Falk and Konold, 1997; Saffran et al., 1996) and chaotic patterns underlying nonlinear systems (e.g., Smithson, 1997). Chater (1996) and Chater and Vitanyi (2003) adopt a monotonic entropy–complexity relation, suggesting that this sort of pattern sensitivity is grounded in a basic cognitive principle: people search for the simplest (i.e., sparsest, most compressed) representation of a given input. This approach operationalizes sparseness or compressibility of a stimulus in terms of Kolmogorov complexity (Kolmogorov, 1965), an information theoretic construct reflecting the length of the shortest computer program that can encode and reproduce the stimulus (e.g., Chater and Vitanyi, 2003). Falk and Konold (1997) provide convincing behavioral support for this perspective in showing that series that are subjectively perceived as more disordered take longer to memorize and are more difficult to copy. Antrobus (1968) furthermore demonstrated that auditory series of greater entropy are associated with fewer task-unrelated thoughts.

While the above studies provide substantial evidence that the brain is sensitive to input entropy, we hypothesized more specifically that certain brain systems would track entropy in a convex manner, indicating sensitivity to complexity. Note that entropy captures only a partial feature of a temporally unfolding environment, namely the uncertainty in the signal generated by a system, rather than specifying the system itself. Researchers in the field of complexity science have quantified "complexity" in terms of the sophistication of a system's underlying structural configuration, whereas entropy captures the randomness or uncertainty associated with a system's output (e.g., Crutchfield, 2012). This formulation of complexity has roots in early work by Huberman and Hogg (1986), which framed complexity in terms of the diversity of interactions among elements of a system across all levels of a system's structural hierarchy. More recent treatments of complexity have followed a similar trajectory: Bialek et al. (2001) emphasized the generalizability of the predictive information captured by models. Crutchfield's structural complexity (Crutchfield, 2012; Feldman et al., 2008) reflects the model sophistication required to specify a system's underlying configuration. Bayesian model selection accounts for complexity in terms of model evidence or marginal likelihood (see Spiegelhalter et al., 2002).

The evidence for a generative model relies on a tradeoff between fit and complexity, where complexity effectively measures the degrees of freedom, in terms of model parameters, needed to provide an accurate explanation of the data. In this sense, entropy represents the degrees of freedom in the data, while complexity captures the degrees of freedom used by the model to explain those data. This resonates with current neurocomputational theories of free energy minimization, where approximate Bayesian inference (e.g., via predictive coding) serves to maximize model accuracy and minimize complexity (Clark, 2012; Friston, 2010). These theories are consistent with the hypothesis that the brain encodes both accuracy and complexity.

Independent of the formal details, these latter approaches to complexity converge on a central principle: systems generating either highly structured or random outputs can often be specified in a relatively concise way — that is, in terms of a model with fewer parameters or succinct schema — while systems characterized by more intricate underlying structural interactions tend toward producing outputs of intermediate entropy and require more sophisticated models. Consequently, there is a convex relationship between entropy and complexity such that complexity is minimal in systems generating outputs with extremely low or high entropy, but is maximal somewhere between these extremes (Gell-Mann, 1995; Huberman and Hogg, 1986; Lopez-Ruiz et al., 1995; Shiner et al., 1999).

The above discussion does not constitute theoretical hairsplitting, as it offers a more detailed account of how the human brain may process sensory inputs of varying disorder. For example, neural sensitivity to varying complexity (a curvilinear response to entropy) may reflect the brain's maintenance of a generative model useful for predicting incoming sensory stimuli by inferring their underlying causes (e.g., Dayan et al., 1995; Friston, 2010). This abstract model of the environment's structural configuration provides a succinct template useful for generalization and for detecting changes between environmental states.[2] Interestingly, behavioral work has shown that stimuli with intermediate levels of randomness are often considered attention-grabbing, or judged as more interesting, aesthetically appealing or otherwise "complicated" (Berlyne, 1971; Loewenstein, 1994; Vitz, 1966). Abdallah and Plumbley (2009) formally demonstrated that series in which each discrete stimulus reduces a relatively large amount of prior uncertainty are characterized by intermediate levels of disorder; this provides a computational explanation for why such stimuli are perceived as highly engaging.

Given this motivation, we hypothesized that the degree of functional integration within specific networks of the human brain would vary according to both the entropy of an ongoing sensory input as well as the complexity of the system generating that input. To test this hypothesis, we used functional MRI to model the whole-brain connectivity networks of several seed regions while participants passively listened to four 2.5 min auditory series. Each series was characterized by a different level of entropy as determined by the transition constraints between tones. We then used planned contrasts to probe for specific entropy-dependent changes in the regression coefficients of the seed time series.

---

[2] To illustrate, a model that represents a system as "transitioning between four states deterministically" is consistent with 24 possible instantiations of actual low-entropy outputs (e.g., *ABCDABCD…* or *DBCADBCA…*). Conversely, a random source that generates a continuous series of four tokens can be represented as, "all state transitions are equally likely." These concise descriptions are insufficient for lossless compression or veridically reproducing any specific stimulus generated by a system, but are indeed sufficient for detecting a change from an ordered to a random environment. Most importantly, although the systems generating these series vary greatly in the expected conditional entropy of their output streams (2 bits in the random case, 0 in the deterministic case), both share concise descriptions when specifying state transitions. In contrast, an output such as *ABCDAABCDABCD…* has a conditional entropy somewhere between the random and deterministic cases above, but the system generating this series itself is more challenging to specify, e.g., "generates ABCD consecutively with the exception that A may repeat itself," and therefore can be considered more complex than the random or deterministic case.

Seed regions used in the connectivity analysis were selected based on numerous prior studies implicating both the anterior cingulate cortex (ACC) and hippocampal formation (HF) in tracking statistical regularities across several modalities and paradigms. The ACC has been reported to track statistical constraints (Harrison et al., 2006; Nastase et al., 2014), as well as mediate implicit expectation (Aarts et al., 2008; Berns et al., 1997; Ursu et al., 2009). The HF has been implicated in coding for statistical properties of stimulus series (Harrison et al., 2006, 2011; Strange et al., 2005), particularly probabilistic associations between sequence elements in statistical learning paradigms (Schapiro et al., 2012, 2014; Turk-Browne et al., 2009, 2010). However, several studies quantifying hippocampal responses to different levels of regularity (Nastase et al., 2014), changes in regularity (Tobia et al., 2012), or violations of regularity in different domains (Bubic et al., 2011) have failed to find hippocampal involvement. Connectivity analysis serves as an alternative tool for probing how the brain processes sensory uncertainty that may capture phenomena not amenable to activation mapping, as mean activity in a region may remain invariant even while connectivity between regions changes across conditions.

Materials and methods

Participants

Twenty right-handed adults (mean age = 29.9 years; standard deviation = 9.6 years; 12 male) participated in the study. Participants reported no history of psychiatric illness, substance abuse, or hearing impairments, and underwent an interview with a board-certified medical doctor prior to scanning to evaluate other exclusion criteria. Data from one participant who completed the study were excluded from further analysis because of excessive movement during the scan. The ethical review board of the University of Trento approved the study.

Design and stimuli

The design consisted of one factor (input entropy) with four levels. In a single MR session, participants were presented with four auditory series, each 2.5 min in length. Tones within the series were presented at a rate of 3.3 Hz. After each series, there was a 22.5 s silent period to allow the hemodynamic response to return to baseline. Series were constructed by sampling from four tone tokens (262 Hz, 294 Hz, 330 Hz, and 394 Hz), controlled for relative token frequency (25%) and the number of self-repetitions (25%). Each auditory series was characterized by one of four levels of Markov (conditional) entropy ranging from random (no constraints) to highly ordered (strong transition constraints). This resulted in four series, each governed by a different level of statistical constraints: random, low, medium, and high. The actual Markov Entropy levels of the four series were 0.81, 1.35 1.56, and 2 (see Fig. 1). Each participant was assigned a different arrangement of series so that there was no relationship between the entropy level of a series and its position in the scanning session. The sounds generated by the EPI sequence were constant across the different conditions and the volume level was adjusted for each subject so that the tones could be heard comfortably over the scanner noise.

Image acquisition and procedure

All data were acquired using a 4T Bruker/Siemens system. Two structural scans per participant were acquired with a 3D T1-weighted MPRAGE sequence (TR/TE = 2700/4 ms, flip angle = 7°, isotropic voxel size = 1 mm, matrix = 256×224; 176 sagittal slices). Functional scans were acquired with a single-shot EPI sequence (TR/TE = 1500/33 ms, flip angle = 75°, voxel size = $4 \times 4 \times 4.8$ mm^3, matrix = 64×64 mm; 25 interleaved slices parallel to AC/PC, slice skip factor = 0.2, 471 volumes, 706.5 s overall scan time). During the fMRI scan, cardiac and respiration data were acquired using a photoplethysmograph

and a respiration belt (Bruker), respectively. Participants lay passively while observing a fixation cross and were instructed to remain wakeful and listen to the auditory stimulus as if they were listening to music at home.

Preprocessing and generation of ROIs

The first 15 EPI volumes were discarded to ensure stabilization of the signal, leaving 456 volumes of functional data. Four 100-volume (150 s) time series corresponding to the 2.5 min of auditory presentation for each of the four conditions were spliced from the single functional run. The functional time series were de-spiked and the cardiac and respiratory data were used for physiological noise correction according to the RETROICOR procedure (Birn et al., 2006; Glover et al., 2000; implemented in AFNI). Motion correction was applied to each of the four time series using AFNI's 3dvolreg utility. Head motion parameters for each subject were visually inspected, their derivatives calculated, and functional volumes with motion in excess of 1 mm were censored in the subsequent regression—this accounted for approximately 1.5% of the data. A 6 mm spatial smoothing kernel was applied to increase the signal-to-noise ratio of the time series.

Participants' structural scans were processed via FreeSurfer (Fischl et al., 2002). First, the two structural scans were averaged to increase the quality of the anatomical image. FreeSurfer's automatic parcellation functionality was used to derive anatomical parcellations of the cortical surface and subcortical regions for each participant. This procedure uses a probabilistic labeling algorithm that incorporates the anatomical conventions of Duvernoy et al. (1991) and is thus based on macroanatomical landmarks, not cytoarchitectonic maps. The anatomical precision of this method is high, approaching that of manual parcellation (Desikan et al., 2006; Fischl et al., 2002, 2004). Using this procedure, bilateral ACC and HF anatomical regions were delineated for each participant. These were verified manually, and then downsampled from the original structural resolution to the functional resolution to serve as anatomical masks. As an additional check, we projected the location of these seed regions to common (Talairach) space in order to inspect the anatomical consensus. Overlap was high across all subjects, indicating good delineation of the anatomical structures. The mean time series of the functional data in the ACC and HF (bilaterally) were then extracted for the purpose of generating whole-brain connectivity maps. This was done in each participant's native acquisition space.

Generation of whole-brain connectivity maps

Prior to conducting the whole-brain connectivity analysis, we evaluated the degree of correlation between the two ACC and two HF time series. Strong correlation between homologous seed time series (as previously documented for resting state data, e.g., Stark et al., 2008) would obviate independent analyses for each seed region. For bilateral ACC, the mean correlation (Pearson's r) across participants exceeded 0.8 in all conditions (mean/SD in the four conditions: 0.83/0.17; 0.86/0.08; 0.84/0.11; 0.86/0.08). Given this high correlation (which exceeded 0.9 in some participants), we used the left ACC time series as a proxy to avoid redundancy. Connectivity between HF homologs was lower (mean/SD in the four conditions: 0.66/0.25; 0.71/0.15; 0.69/0.20; 0.72/0.20); thus the right and left HF seeds were examined separately. Correlations between ACC and HF time series were low, not exceeding 0.5 in any case.

At the individual-participant level, whole-brain connectivity maps were constructed by using a seed region's time series as the regressor of interest in a multiple regression implemented via AFNI's 3dDeconvolve utility. In addition to the seed time series, nuisance regressors included a linear trend regressor for modeling scanner drift and six motion parameters. On the individual-participant level, connectivity in each condition was quantified as the regression coefficient (beta parameter) for the seed time series for a given voxel, after accounting for the
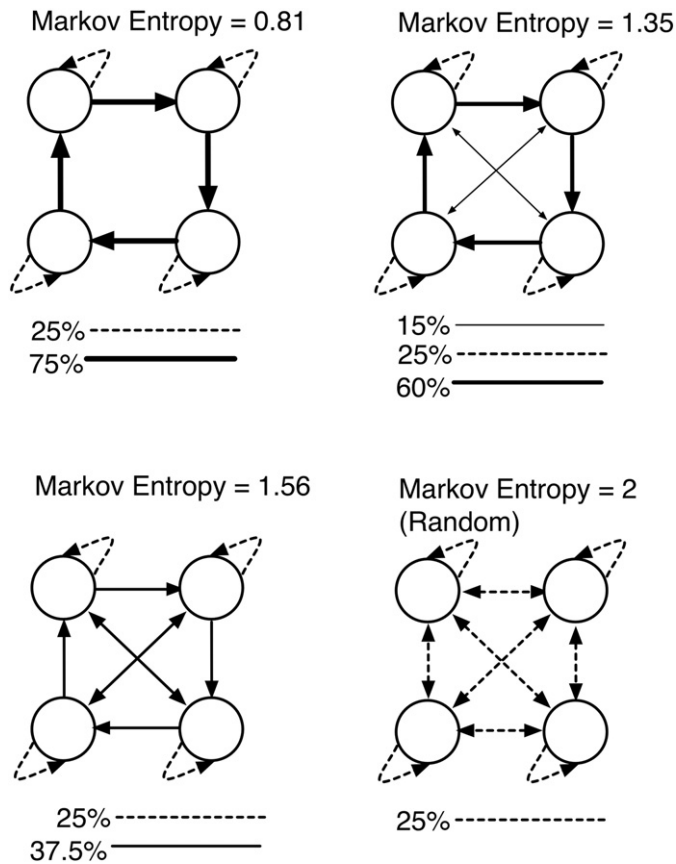
Fig. 1. Markov chains used to construct the four tonal series used in the study. Markov entropy defines the overall degree of transition constraints, with higher entropy indicating weaker constraints. The series consisted of a repeated sampling of four tones, presented according to such constraints. For a four-state series, Markov entropy of 2 is maximal. Strength of transition constraints is indicated via line types under each graph. The proportion of self-repetitions was maintained at 25% across all conditions and the marginal frequency of each state was held at 25% across conditions as well. Thus, the conditions differed only in their transition structure.

nuisance regressors (see Friston, 1994, Friston et al., 1997, for a similar approach). The connectivity analysis returned 12 whole-brain connectivity maps per participant: 4 entropy levels × 3 seed regions. These maps were aligned to a common template space for group level analysis as follows. First, each participant's structural image was aligned to the same spatial reference point as the participant's functional scans (using AFNI's align_epi_anat.py function). The resulting aligned structural image was then aligned to the MNI 152 template in Talairach space using a 12-parameter affine transformation. The transformation matrix generated in this last step was applied to the participant's statistical maps. All spatial registration steps were inspected and manually adjusted if needed.

For the group level analysis, connectivity maps for each seed region were analyzed separately. For each seed region, each voxel's data were analyzed using planned contrast coefficients (linear-polynomial and quadratic-polynomial; Büchel et al., 1998; sometimes referred to as "trend analysis"). The linear contrast weights were $-3, -1, 1, 3$ and the quadratic contrast weights were $-1, 1, 1, -1$. This is a standard procedure for testing specific hypotheses using contrast weights (see Quinn and Keough, 2002, Ch. 8), where the sum of squared error (SS) for the group (SS_{Group}) is partitioned into SS_{Linear}, $SS_{Quadratic}$ and so on, each with one degree of freedom. For each voxel, the procedure returned a t-value for each contrast reflecting its statistical significance. The single voxel threshold for these t-statistic maps was set at $p < .005$, corrected for multiple comparisons (family-wise error alpha level =

.05) using cluster-extent thresholding (Forman et al., 1995). We could thus identify clusters where the strength of connectivity with a given seed showed a statistically significant linear trend or quadratic trend across the four entropy conditions. We did not test for a cubic trend as we had no a priori hypothesis corresponding to this contrast. Note also that these two contrasts are not mutually exclusive and a single cluster might exhibit statistically significant t-values for both linear and quadratic contrasts, although this did not occur in practice.

Results

Autonomic indices during the scan

There was no indication that the experimental manipulation affected autonomic (cardiac and respiratory) indices recorded during scanning. The mean heart rate in all condition was 62-63 BPM (mean/SD for highest to lowest entropy condition: 62.7/9.5; 62.3/8.6; 62.7/10.1; 62.5/92). Heart rate variance was also highly similar across conditions (arbitrary units, all values within 49–50). The removal of instantaneous cardiac and respiratory effects from the BOLD data and the fact that autonomic indices were highly similar across conditions strongly suggest that any differences in connectivity were not due to potential confounds between autonomic state and input entropy.

Linear and quadratic connectivity profiles

The contrast analysis applied voxelwise linear and quadratic contrast weights at the group level to identify voxels showing a linear relation between connectivity and entropy, and/or a quadratic (curvilinear) relationship between connectivity and entropy, i.e., differentiating levels of complexity. Of the four possible connectivity profiles — positive/negative linear relations and U-shaped/inverse U-shaped curvilinear relations — only two profiles were reliably identified in the data. These were (1) stronger connectivity for auditory series of greater regularity (i.e., a negative linear relation between connectivity and series entropy), and (2) a convex, inverted U-shaped relation indicating stronger connectivity for intermediate levels of disorder (increased connectivity for greater complexity).

The linear relation, which in every case reflected increased connectivity for more structured (lower entropy) series, was associated with very different connectivity maps for the ACC and HF seed regions, as might be expected given the relatively low correlations between the seed time series for these regions. As shown in Fig. 2 and Table 1, for ACC, the regions identified were a right-hemisphere cluster encompassing the precentral and postcentral gyri, medial frontal gyrus and inferior frontal gyrus, a left middle frontal cluster extending to the postcentral gyrus, bilateral posterior middle temporal clusters, and a left parahippocampal cluster.

For the left and right HF seed regions (Fig. 2; Tables 2 and 3), the regions identified by the linear contrast were largely subcortical, with extensive basal ganglia (lentiform nucleus and putamen) clusters identified bilaterally for both left and right HF. Contralateral connectivity between the right HF and the left middle frontal gyrus was also linearly modulated by input disorder, as well as connectivity with the right posterior superior temporal gyrus and bilateral cerebellum. Left HF connectivity scaled linearly with a right inferior parietal cluster, a left middle frontal cluster, the left insula and the right cerebellum.

Regions exhibiting convex, inverted U-shaped connectivity profiles were found for all three seed regions (Fig. 2; Table 4). For the left ACC seed, connectivity was greatest at intermediate levels of entropy for bilateral precuneus clusters. For the right HF, clusters comprising the right ACC, left cingulate, left medial frontal gyrus, and right cerebellum adhered to convex connectivity profiles. Finally, the left HF demonstrated a curvilinear connectivity profile with the contralateral midcingulate.

Discussion

An emerging theme in current cognitive and neurobiological work is that the brain codes for uncertainty, or entropy, in sensory data in order to actively predict forthcoming input and guide adaptive behavior (Clark, 2012; Friston, 2010). This provides strong motivation for research paradigms aimed at identifying neural mechanisms coding for environmental uncertainty. Prior work in psychology has also suggested that algorithmic complexity — which converges with entropy for increasingly random stimuli — may capture pattern-seeking behavior and how organisms efficiently encode complex stimuli (Chater and

Vitanyi, 2003). The current study contributes to this line of work by showing that connectivity among a variety of brain regions not only tracks uncertainty, but also varies in a manner consistent with a curvilinear relation between entropy and structural/model complexity. These findings provide support for our hypothesis that the human brain tracks both the entropy of environmental signals, and the complexity of the system generating those signals.

Beyond demonstrating that the brain tracks these orthogonal features of an input, a striking result was that, of the four possible connectivity profiles relating uncertainty to connectivity, only two occurred reliably. These were a negative linear relation between connectivity and
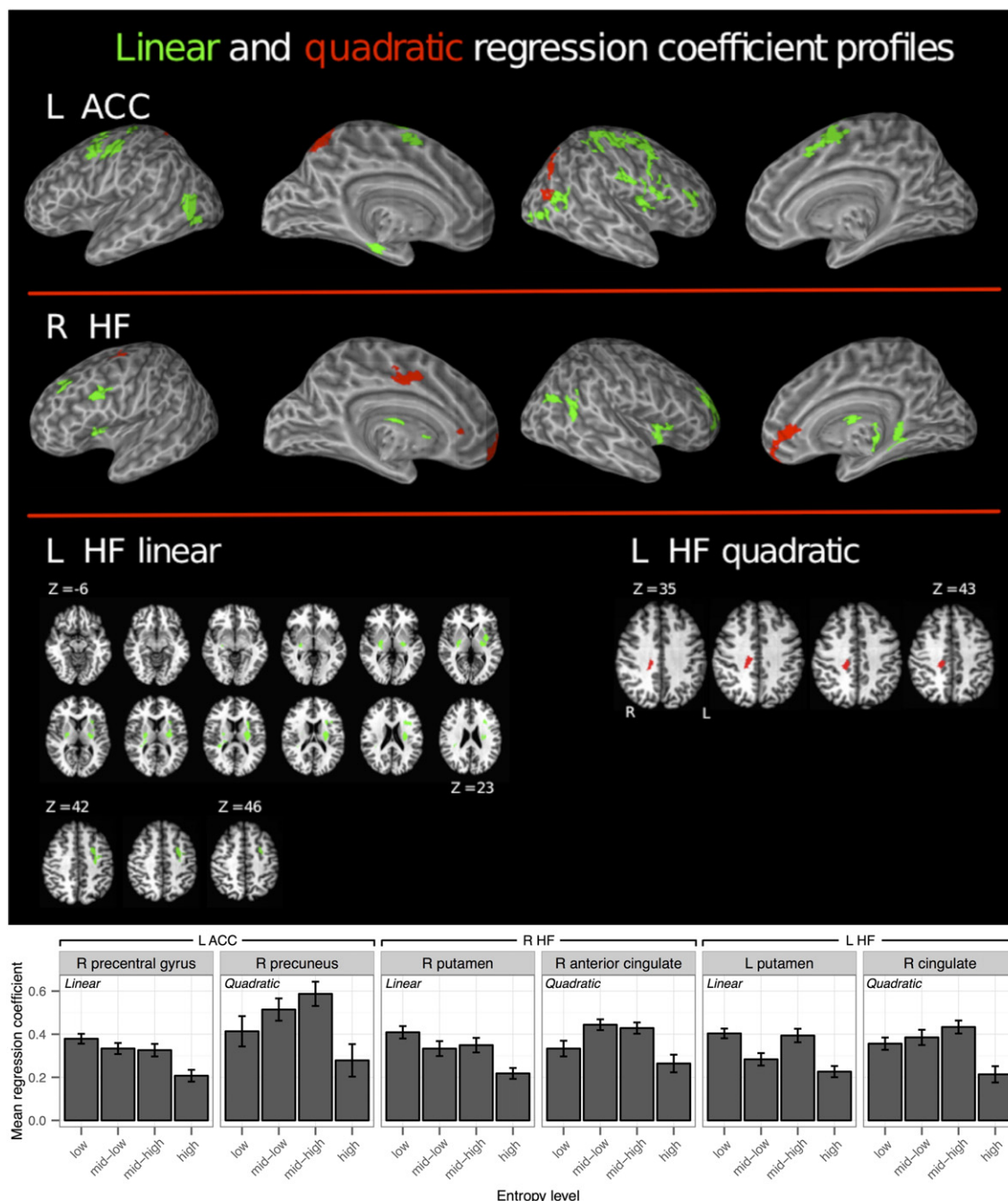

Fig. 2. Linear and quadratic entropy-related connectivity maps, where clusters defined by a significant linear trend (connectivity profile) are displayed in green and clusters defined by a significant quadratic (inverted U-shaped) trend are displayed in red. Connectivity maps are plotted for each of the three seed regions, left ACC, right HF, and left HF. Connectivity is quantified by the regression coefficient of the seed time series in the regression model. Results are projected to the cortical surface in cases where this aids visualization. The voxel-wise threshold was set at $p < .005$, further corrected for multiple comparisons using cluster-extent constraints (FWE < .05). In the bottom panel, connectivity profiles from six representative clusters are plotted with error bars depicting within-participants standard error around the mean regression coefficient across subjects (Loftus and Masson, 1994). Connectivity profiles from two clusters (one linear trend, one quadratic trend) are plotted for each seed region.

Table 1

Left ACC seed region. Clusters (labeled according to center of mass) where connectivity decreases monotonically with increasing input entropy.

	Talairach coordinates (center of mass)			Volume (mm³)	T (max.)
	x	y	z		
Left ACC					
R precentral gyrus	35.3	−18.2	48.0	9016	−4.885
L middle frontal gyrus	−29.1	−13.1	47.1	5543	−5.117
R postcentral gyrus	49.0	−7.9	19.8	1800	−4.282
L middle temporal gyrus	−43.2	−60.9	3.0	940	−4.640
R middle temporal gyrus	45.9	−64.1	4.0	938	−4.509
R precentral gyrus	55.9	7.1	8.7	863	−4.806
R medial frontal gyrus	6.2	−3.1	51.4	859	−4.265
R inferior frontal gyrus	48.4	25.1	19.6	676	−4.667
L parahippocampal gyrus	−20.4	−18.6	−16.6	665	−5.060

input entropy (stronger connectivity associated with greater statistical regularity), and an inverse U-shaped profile indicating increased connectivity for intermediate levels of disorder. Another observation is that each of the seed regions concurrently displayed both linear and convex connectivity profiles with certain brain regions. This suggests that both the ACC and HF discriminate entropy and complexity levels via their connectivity with other structures.

These two connectivity profiles lend themselves to distinct functional interpretations. Neural systems in which connectivity linearly tracks input entropy are interpreted to be involved in coding for statistical regularities in the input itself or in filtering stochastic input in the context of predictive or efficient coding strategies (e.g., computing prediction error). Conversely, numerous theoretical treatments have suggested that complexity is a measure of the model sophistication required to specify a system's behavior (Bialek et al., 2001; Crutchfield et al., 2009; Huberman and Hogg, 1986; Rissanen, 1986; Spiegelhalter et al., 2002). Accordingly, we suggest that neural systems in which connectivity is greatest for intermediate levels of entropy may mediate the passive, online maintenance of an internal model of a stimulus' generator(s), i.e., a generative model used to predict incoming sensory data (Friston, 2010; Gentner and Stevens, 1983; Johnson-Laird, 1983; Roger and Ashby, 1970). This connectivity profile reflects the increased computational demands typically associated with modeling systems of intermediate entropy.

The finding that connectivity strength tracks input complexity is consistent with MEG work by Patel and Balaban (2000), who measured magnetoencephalographic signals while participants listened to series of tones ranging in statistical structure from random to deterministic scale-like sequences. Synchronization between MEG sensors was shown to be generally weaker in the random condition and exhibited an inverse U-shaped coherence profile, such that the strongest interregional synchrony was found for the more melodic fractal ($1/f$ and $1/f^2$) patterns. In related work at the interface of complexity science and computational music analysis, Abdallah and Plumbley (2009) proposed a

Table 3

Left HF seed region. Clusters where connectivity decreases monotonically with increasing input entropy.

	Talairach coordinates (center of mass)			Volume (mm³)	T (max.)
	x	y	z		
Left HF					
L lentiform/putamen	−26	−12	13	3242	−5.15
R lentiform/putamen	25	−15	7	1401	−4.72
R inferior parietal lobule	33	−26	27	1286	−5.34
L insula	−29	13	17	1001	−4.64
L middle frontal gyrus	−26	−3	44	760	−4.31
R cerebellum	8	−64	−28	645	−4.64

measure called predictive information rate (PIR) to account for convex responses to entropy. This metric, which is closely related to previously mentioned measures of complexity (Abdallah and Plumbley, 2011), quantifies the additional amount of predictive information provided by a stimulus at time t about what may occur at $t + 1$ in comparison to what could have been predicted about $t + 1$ based on $t − 1$ alone. This "additional amount of information" conveyed by the present stimulus is minimal in completely random and completely deterministic contexts—thus preserving both the curvilinear relation between entropy and complexity and capturing the commonly found inverted U-shaped relation between entropy and subjective judgments of aesthetic value or appeal (Berlyne, 1971). PIR, when used to analyze samples of minimalist musical pieces by Philip Glass, was highly consistent with structural analyses by expert human listeners. This work provides a compelling framework in which to interpret our findings and highlights the possibility that neural substrates sensitive to system complexity may also be linked to such qualitative human judgments as melodic quality or aesthetic appeal (Vitz, 1966; see Kintsch, 2012, for a recent theoretical review).

Beyond the implications of our results for theories of complexity and the coding of disorder, our findings have specific implications for the current understanding of ACC and HF function. These seed regions were selected based on a literature documenting their differential activity in response to manipulations of statistical regularity (e.g., Harrison et al., 2006; Turk-Browne et al., 2009). Importantly, our results demonstrate that the degree to which these regions are functionally coupled to particular networks varies with sensory uncertainty. Prior work has shown that ACC connectivity fluctuates in tandem with external conflict demands and has implicated a highly similar network of regions to those found here (Fan et al., 2008). Fan et al. (2008) examined whole-brain connectivity of rostral ACC during performance of a congruent or incongruent flanker task, revealing increased functional connectivity between ACC and numerous regions during the *in*congruent, conflict-inducing condition. The regions identified by Fan et al. (2008) are highly consistent with the regions in our study showing increased correlation

Table 4

Clusters where connectivity tracks complexity for left ACC, left and right HF.

	Talairach coordinates (center of mass)			Volume (mm³)	T (max.)
	x	y	z		
Left ACC					
R precuneus	36.3	−69.5	37.0	1626	−4.264
L precuneus	−10.2	−59.9	51.3	1472	−3.932
Left HF					
R cingulate gyrus	15	−27	38	791	−4.64
Right HF					
R anterior cingulate	13	40	0	1510	−4.33
R cerebellum	18	−63	−44	1371	−4.34
L cingulate gyrus	−17	−12	41	725	−4.60
L medial frontal gyrus	−8	54	1	722	−4.09

Table 2

Right HF seed region. Clusters where connectivity decreases monotonically with increasing input entropy.

	Talairach coordinates (center of mass)			Volume (mm³)	T (max.)
	x	y	z		
Right HF					
R putamen	25	−4	9	4114	−5.47
L lentiform/putamen	−25	1	16	3581	−5.43
R middle frontal gyrus	32	45	22	2498	−5.13
R cerebellum	32	−36	−30	1783	−5.33
L cerebellum	−32	−46	−35	1117	−5.22
R thalamus	10	−28	0	877	−4.71
R superior temporal gyrus	44	−54	17	747	−4.1

with ACC for series with greater statistical constraints (see Table 1). Fan et al. (2008) suggested that this connectivity pattern reflects response facilitation in the presence of conflicting flanker stimuli. Our results however suggest that this connectivity profile reflects endogenous sensitivity to the predictability of a stimulus, given the lack of exogenous conflict or response evaluation in our paradigm. In series with greater statistical structure, each element was highly informative of the following element, thus licensing predictive processing. This predictive coding account is supported by work showing that ACC activity may be directly linked to preparatory activity occurring prior to target presentation (Schulz et al., 2011), and suggests that the "prediction of response-outcome" model of medial prefrontal cortex should be expanded to include implicit perceptual inference, where no explicit response is required (Alexander and Brown, 2011; Ferdinand et al., 2012).

For both left and right HF seed regions, increased connectivity with large portions of bilateral putamen was found in response to series with stronger statistical constraints. These results are consistent with reports that both medial temporal lobe structures and the basal ganglia are involved in implicit sequence learning and artificial grammar learning (Forkstam and Petersson, 2005; Rauch et al., 1997; Schendan et al., 2003). Furthermore, recent work suggests that the putamen codes for probabilistic associations (in reinforcement learning paradigms; Haruno and Kawato, 2006) and temporal predictions in the auditory domain (Geiser et al., 2012; Grahn and Rowe, 2013). While determining which of the two regions drives the other was outside the scope of the current work, our results suggest that statistically structured inputs spontaneously synchronize these structures. Importantly, regions whose effective connectivity with the HF adhered to this connectivity profile were very distinct from those associated with HF resting state functional connectivity (Vincent et al., 2006). Whether HF and ACC mediate similar functions for non-auditory inputs is an open question, as our prior work suggests that different systems code for statistical features of inputs in different sensory modalities (Nastase et al., 2014).

Of particular interest is the finding that connectivity between ACC and bilateral precuneus clusters tracked environmental complexity. The precuneus has been implicated in the maintenance of internal representations (Cavanna and Trimble, 2006; Fletcher et al., 1995; Wagner et al., 2005; Wolpert et al., 1998), while connectivity between ACC and posterior midline structures correlates with working memory performance (Hampson et al., 2006). Increased connectivity between HF seed regions and ventromedial prefrontal cortex, midcingulate and medial frontal gyri was found for series of intermediate disorder. Importantly, these areas overlap with both the default mode network (Buckner et al., 2008; Greicius et al., 2003; Raichle et al, 2001) and regions involved in prospective simulation (Buckner and Carroll, 2007). Our findings inform this line of work by demonstrating that, in the absence of any explicit task, the connectivity of these default regions is spontaneously modulated by the degree of structure in the sensory milieu. Some advocates of the default mode hypothesis have suggested that correlated, task-independent activity in the precuneus and ACC — in addition to other typical default mode structures — reflects the maintenance of an internal, probabilistic model of the environment (Raichle and Gusnard, 2005; Rogers et al., 2010). Our findings suggest that changes in the whole-brain connectivity of ACC and HF reflect a passive, rudimentary modeling operation in which internal representations are maintained or refined online, separate from low-level sensory processing.

We used a listening paradigm that lacked an observable behavioral component, a decision motivated by evidence that explicitly tracking sequential structure fundamentally affects both learning and neural responses, including functional connectivity (Fletcher et al., 2005). We opted for this approach with the intention of isolating a perceptual, or "background" process that operates by default, in absence of any particular behavior or task. This approach also allows our results to better interface with findings in the resting state functional connectivity literature. For this reason, these data cannot directly speak to the impact of sensory regularities on behavior *per se*, or how our stimuli affected attentional demands. As explanatory constructs, attention, expectation and prediction are tightly linked (Summerfield and Egner, 2009; Zhao et al., 2013). From a phenomenological perspective, it could be that auditory series at certain levels of entropy were simply more interesting, thus drawing more attention. That is, attention could be a moderator accounting for part of the variance in either the monotonic or quadratic relations (though by definition not both) observed between stimulus entropy and the strength of connectivity. This interpretation would be consistent with early work reporting fewer task-unrelated thoughts in the context of greater-entropy auditory stimulation (Antrobus, 1968), indicating an effect of sensory regularity on either attentional deployment or systems mediating mind-wandering.

Future work may also investigate the relationship between input entropy and effective connectivity in lower-level auditory areas. This particular topic of inquiry is complicated by the substantial functional heterogeneity of primary and secondary auditory cortices. We have previously shown that small, adjacent regions of the supratemporal plane have highly divergent response profiles to input entropy (Tremblay et al., 2012). Presently, our choice of ACC and HF as seed regions in the current study was based on repeated demonstrations that these regions serve in tracking uncertainty or predictive processing.

Summary

To conclude, the way in which ACC and HF interface with other brain areas suggests two functionally distinct operations taking place concurrently. Interactions between the hippocampus and basal ganglia, as well as a network including ACC and bilateral precentral regions, track input entropy directly. On the other hand, the inverse U-shaped connectivity profile associated with midline, default mode structures suggests that their function, though related to input statistics, is more abstract: this connectivity profile does not translate into a direct relation with input disorder and cannot be said to track the mean predictability of series elements or the degree to which they license prediction. Instead, consistent with current approaches in complexity science, we suggest that this system may be involved in spontaneously constructing and maintaining an internal probabilistic model of the environmental configuration driving sensory input rather than tracking the input *per se*. While the random and highly structured conditions are trivial to model, inputs of intermediate entropy are more computationally demanding to model and thus engage these midline structures to a greater extent. Specifying the detailed computations carried out in the regions identified here, as well as expanding the scope of the stimuli that drive these operations, are well-defined research questions for future studies.

References

Aarts, E., Roelofs, A., van Turennout, M., 2008. Anticipatory activity in anterior cingulate cortex can be independent of conflict and error likelihood. J. Neurosci. 28, 4671–4678.

Abdallah, S.A., Plumbley, M.D., 2009. Information dynamics: patterns of expectation and surprise in the perception of music. Connect. Sci. 21, 89–117.

Abdallah, S.A., Plumbley, M.D., 2011. A measure of statistical complexity based on predictive information with application to finite spin systems. Phys. Lett. A 376, 275–281.

Alexander, W.H., Brown, J.W., 2011. Medial prefrontal cortex as an action-outcome predictor. Nat. Neurosci. 14, 1338–1344.

Antrobus, J.S., 1968. Information theory and stimulus-independent thought. Br. J. Psychol. 59, 423–430.

Ashby, W.R., 1947. Principles of the self-organizing dynamic system. J. Gen. Psychol. 37, 125–128.

Barlow, H.B., 1961. Possible principles underlying the transformation of sensory messages. In: Rosenblith, W.A. (Ed.), Sensory Communication. MIT Press, Cambridge, pp. 217–234.

Berlyne, D.E., 1957. Conflict and information-theory variables as determinants of human perceptual curiosity. J. Exp. Psychol. 53, 399–404.

Berlyne, D.E., 1971. Aesthetics and Psychobiology. Appleton-Century-Crofts, New York.

Berns, G.S., Cohen, J.D., Mintun, M.A., 1997. Brain regions responsive to novelty in the absence of awareness. Science 276, 1272–1275.

Bialek, W., Nemenman, I., Tishby, N., 2001. Predictability, complexity, and learning. Neural Comput. 13, 2409–2463.

Birn, R.M., Diamond, J.B., Smith, M.A., Bandettini, P.A., 2006. Separating respiratory-variation-related fluctuations from neuronal-activity-related fluctuations in fMRI. Neuroimage 31, 1536–1548.

Bischoff-Grethe, A., Proper, S.M., Mao, H., Daniels, K.A., Berns, G.S., 2000. Conscious and unconscious processing of nonverbal predictability in Wernicke's area. J. Neurosci. 20, 1975–1981.

Borst, A., Theunissen, F.E., 1999. Information theory and neural coding. Nat. Neurosci. 2, 947–957.

Brady, T.F., Konkle, T., Alvarez, G.A., 2009. Compression in visual working memory: using statistical regularities to form more efficient memory representations. J. Exp. Psychol. Gen. 138, 487–502.

Bubic, A., von Cramon, D.Y., Schubotz, R.I., 2011. Exploring the detection of associatively novel events using fMRI. Hum. Brain Mapp. 32, 370–381.

Büchel, C., Holmes, A., Rees, G., Friston, K., 1998. Characterizing stimulus–response functions using nonlinear regressors in parametric fMRI experiments. Neuroimage 8, 140–148.

Buckner, R.L., Carroll, D.C., 2007. Self-projection and the brain. Trends Cogn. Sci. 11, 49–57.

Buckner, R.L., Andrews-Hanna, J.R., Schacter, D.L., 2008. The brain's default network. Ann. N. Y. Acad. Sci. 1124, 1–38.

Buiatti, M., Pena, M., Dehaene-Lambertz, G., 2009. Investigating the neural correlates of continuous speech computation with frequency-tagged neuroelectric responses. Neuroimage 44, 509–519.

Cavanna, A.E., Trimble, M.R., 2006. The precuneus: a review of its functional anatomy and behavioural correlates. Brain 129, 564–583.

Chater, N., 1996. Reconciling simplicity and likelihood principles in perceptual organization. Psychol. Rev. 103, 566–581.

Chater, N., Vitanyi, P., 2003. Simplicity: a unifying principle in cognitive science? Trends Cogn. Sci. 7, 19–22.

Clark, A., 2012. Whatever next? Predictive brains, situated agents, and the future of cognitive science. Behav. Brain Sci. 36, 181–204.

Crutchfield, J.P., 2012. Between order and chaos. Nat. Phys. 8, 17–24.

Crutchfield, J.P., Ellison, C.J., Mahoney, J., 2009. Time's barbed arrow: irreversibility, crypticity, and stored information. Phys. Rev. Lett. 103, 094101.

Dayan, P., Hinton, G.E., Neal, R.M., Zemel, R.S., 1995. The helmholtz machine. Neural Comput. 7, 889–904.

Desikan, R.S., Ségonne, F., Fischl, B., Quinn, B.T., Dickerson, B.C., Blacker, D., Buckner, R.L., Dale, A.M., Maguire, R.P., Hyman, B.T., Albert, M.S., Killiany, R.J., 2006. An automated labeling system for subdividing the human cerebral cortex on MRI scans into gyral based regions of interest. Neuroimage 31, 968–980.

Duvernoy, H.M., Cabanis, E.A., Bourgouin, P., 1991. The Human Brain: Surface, Three-Dimensional Sectional Anatomy and MRI. Springer-Verlag, Wien.

Falk, R., Konold, C., 1997. Making sense of randomness: implicit encoding as a basis for judgment. Psychol. Rev. 104, 301–318.

Fan, J., Hof, P.R., Guise, K.G., Fossella, J.A., Posner, M.I., 2008. The functional integration of the anterior cingulate cortex during conflict processing. Cereb. Cortex 18, 796–805.

Feldman, D.P., McTague, C.S., Crutchfield, J.P., 2008. The organization of intrinsic computation: complexity–entropy diagrams and the diversity of natural information processing. Chaos 18, 043106.

Ferdinand, N.K., Mecklinger, A., Kray, J., Gehring, W.J., 2012. The processing of unexpected positive response outcomes in the mediofrontal cortex. J. Neurosci. 32, 12087–12092.

Fischl, B., Salat, D.H., Busa, E., Albert, M., Dieterich, M., Haselgrove, C., van der Kouwe, A., Killiany, R., Kennedy, D., Klaveness, S., Montillo, A., Makris, N., Rosen, B., Dale, A.M., 2002. Whole brain segmentation: automated labeling of neuroanatomical structures in the human brain. Neuron 33, 341–355.

Fischl, B., van der Kouwe, A., Destrieux, C., Halgren, E., Ségonne, F., Salat, D.H., Busa, E., Seidman, L.J., Goldstein, J., Kennedy, D., Caviness, V., Makris, N., Rosen, B., Dale, A.M., 2004. Automatically parcellating the human cerebral cortex. Cereb. Cortex 14, 11–22.

Fletcher, P.C., Frith, C.D., Baker, S.C., Shallice, T., Frackowiak, R.S., Dolan, R.J., 1995. The mind's eye—precuneus activation in memory-related imagery. Neuroimage 2, 195–200.

Fletcher, P.C., Zafiris, O., Frith, C.D., Honey, R.A., Corlett, P.R., Zilles, K., Fink, G.R., 2005. On the benefits of not trying: brain activity and connectivity reflecting the interactions of explicit and implicit sequence learning. Cereb. Cortex 15, 1002–1015.

Forkstam, C., Petersson, K.M., 2005. Towards an explicit account of implicit learning. Curr. Opin. Neurol. 18, 435–441.

Forman, S.D., Cohen, J.D., Fitzgerald, M., Eddy, W.F., Mintun, M.A., Noll, D.C., 1995. Improved assessment of significant activation in functional magnetic resonance imaging (fMRI): use of a cluster-size threshold. Magn. Reson. Med. 33, 636–647.

Friston, K.J., 1994. Functional and effective connectivity in neuroimaging: a synthesis. Hum. Brain Mapp. 2, 56–78.

Friston, K., 2010. The free-energy principle: a unified brain theory? Nat. Rev. Neurosci. 11, 127–138.

Friston, K.J., Buechel, C., Fink, G.R., Morris, J., Rolls, E., Dolan, R.J., 1997. Psychophysiological and modulatory interactions in neuroimaging. Neuroimage 6, 218–229.

Geiser, E., Notter, M., Gabrieli, J.D., 2012. A corticostriatal neural system enhances auditory perception through temporal context processing. J. Neurosci. 32, 6177–6182.

Gell-Mann, M., 1995. The Quark and the Jaguar: Adventures in the Simple and the Complex. St. Martin's Griffin, New York.

Gentner, D., Stevens, A.L., 1983. Mental Models. Erlbaum, Hillsdale.

Glover, G.H., Li, T.Q., Ress, D., 2000. Image-based method for retrospective correction of physiological motion effects in fMRI: RETROICOR. Magn. Reson. Med. 44, 162–167.

Grahn, J.A., Rowe, J.B., 2013. Finding and feeling the musical beat: striatal dissociations between detection and prediction of regularity. Cereb. Cortex 23, 913–921.

Greicius, M.D., Krasnow, B., Reiss, A.L., Menon, V., 2003. Functional connectivity in the resting brain: a network analysis of the default mode hypothesis. Proc. Natl. Acad. Sci. U. S. A. 100, 253–258.

Hampson, M., Driesen, N.R., Skudlarski, P., Gore, J.C., Constable, R.T., 2006. Brain connectivity related to working memory performance. J. Neurosci. 26, 13338–13343.

Harrison, L.M., Duggins, A., Friston, K.J., 2006. Encoding uncertainty in the hippocampus. Neural Netw. 19, 535–546.

Harrison, L.M., Bestmann, S., Rosa, M.J., Penny, W., Green, G.G., 2011. Time scales of representation in the human brain: weighing past information to predict future events. Front. Hum. Neurosci. 5, 37.

Haruno, M., Kawato, M., 2006. Different neural correlates of reward expectation and reward expectation error in the putamen and caudate nucleus during stimulus-action-reward association learning. J. Neurophysiol. 95, 948–959.

Huberman, B.A., Hogg, T., 1986. Complexity and adaptation. Physica D 22, 376–384.

Johnson-Laird, P.N., 1983. Mental Models: Towards a Cognitive Science of Language, Inference, and Consciousness. Harvard University Press, Cambridge.

Kiebel, S.J., Daunizeau, J., Friston, K.J., 2008. A hierarchy of time-scales and the brain. PLoS Comput. Biol. 4, e1000209.

Kintsch, W., 2012. Musings about beauty. Cogn. Sci. 36, 635–654.

Kolmogorov, A.N., 1965. Three approaches to the quantitative definition of information. Probl. Inf. Transm. 1, 3–11.

Loewenstein, G., 1994. The psychology of curiosity: a review and reinterpretation. Psychol. Bull. 116, 75–98.

Loftus, G.R., Masson, M.E., 1994. Using confidence intervals in within-subject designs. Psychon. Bull. Rev. 1, 476–490.

Lopez-Ruiz, R., Mancini, H., Calbet, X., 1995. A statistical measure of complexity. Phys. Lett. A 209, 321–326.

Nastase, S., Iacovella, V., Hasson, U., 2014. Uncertainty in visual and auditory series is coded by modality-general and modality-specific neural systems. Hum. Brain Mapp. 35, 1111–1128.

Olshausen, B.A., Field, D.J., 1996. Emergence of simple-cell receptive field properties by learning a sparse code for natural images. Nature 381, 607–609.

Patel, A.D., Balaban, E., 2000. Temporal patterns of human cortical activity reflect tone sequence structure. Nature 404, 80–84.

Quinn, G.P., Keough, M.J., 2002. Experimental Design and Data Analysis for Biologists. Cambridge University Press, Cambridge.

Raichle, M.E., Gusnard, D.A., 2005. Intrinsic brain activity sets the stage for expression of motivated behavior. J. Comp. Neurol. 493, 167–176.

Raichle, M.E., MacLeod, A.M., Snyder, A.Z., Powers, W.J., Gusnard, D.A., Shulman, G.L., 2001. A default mode of brain function. Proc. Natl. Acad. Sci. U. S. A. 98, 676–682.

Rauch, S.L., Whalen, P.J., Savage, C.R., Curran, T., Kendrick, A., Brown, H.D., Bush, G., Breiter, H.C., Rosen, B.R., 1997. Striatal recruitment during an implicit sequence learning task as measured by functional magnetic resonance imaging. Hum. Brain Mapp. 5, 124–132.

Rissanen, J., 1986. Stochastic complexity and modeling. Ann. Stat. 14, 1080–1100.

Roger, C.C., Ashby, W.R., 1970. Every good regulator of a system must be a model of that system. Int. J. Syst. Sci. 1, 89–97.

Rogers, B.P., Avery, S.N., Heckers, S., 2010. Internal representation of hierarchical sequences involves the default network. BMC Neurosci. 11, 54.

Saffran, J.R., Aslin, R.N., Newport, E.L., 1996. Statistical learning by 8-month-old infants. Science 274, 1926–1928.

Schapiro, A.C., Kustner, L.V., Turk-Browne, N.B., 2012. Shaping of object representations in the human medial temporal lobe based on temporal regularities. Curr. Biol. 22, 1622–1627.

Schapiro, A.C., Gregory, E., Landau, B., McCloskey, M., Turk-Browne, N.B., 2014. The necessity of the medial temporal lobe for statistical learning. J. Cogn. Neurosci. 26, 1736–1747.

Schendan, H.E., Searl, M.M., Melrose, R.J., Stern, C.E., 2003. An fMRI study of the role of the medial temporal lobe in implicit and explicit sequence learning. Neuron 37, 1013–1025.

Schulz, K.P., Bedard, A.C., Czarnecki, R., Fan, J., 2011. Preparatory activity and connectivity in dorsal anterior cingulate cortex for cognitive control. Neuroimage 57, 242–250.

Shiner, J.S., Davison, M., Landsberg, P.T., 1999. Simple measure for complexity. Phys. Rev. E. 59, 1459–1464.

Smithson, M., 1997. Judgment under chaos. Organ. Behav. Hum. Dec. 69, 59–66.

Spiegelhalter, D.J., Best, N.G., Carlin, B.P., Van Der Linde, A., 2002. Bayesian measures of model complexity and fit. J. Roy. Stat. Sci. B 64, 583–639.

Stark, D.E., Margulies, D.S., Shehzad, Z.E., Reiss, P., Kelly, A.M., Uddin, L.Q., Gee, D.G., Roy, A.K., Banich, M.T., Castellanos, F.X., Milham, M.P., 2008. Regional variation in interhemispheric coordination of intrinsic hemodynamic fluctuations. J. Neurosci. 28, 13754–13764.

Strange, B.A., Duggins, A., Penny, W., Dolan, R.J., Friston, K.J., 2005. Information theory, novelty and hippocampal responses: unpredicted or unpredictable? Neural Netw. 18, 225–230.

Summerfield, C., Egner, T., 2009. Expectation (and attention) in visual cognition. Trends Cogn. Sci. 13, 403–409.

Tobia, M.J., Iacovella, V., Hasson, U., 2012. Multiple sensitivity profiles to diversity and transition structure in non-stationary input. Neuroimage 60, 991–1005.

Tremblay, P., Baroni, M., Hasson, U., 2012. Processing of speech and non-speech sounds in the supratemporal plane: auditory input preference does not predict sensitivity to statistical structure. Neuroimage 66, 318–332.

Turk-Browne, N.B., Scholl, B.J., Chun, M.M., Johnson, M.K., 2009. Neural evidence of statistical learning: efficient detection of visual regularities without awareness. J. Cogn. Neurosci. 21, 1934–1945.

Turk-Browne, N.B., Scholl, B.J., Johnson, M.K., Chun, M.M., 2010. Implicit perceptual anticipation triggered by statistical learning. J. Neurosci. 30, 11177–11187.

Ursu, S., Clark, K.A., Aizenstein, H.J., Stenger, V.A., Carter, C.S., 2009. Conflict-related activity in the caudal anterior cingulate cortex in the absence of awareness. Biol. Psychol. 80, 279–286.

Vincent, J.L., Snyder, A.Z., Fox, M.D., Shannon, B.J., Andrews, J.R., Raichle, M.E., Buckner, R.L., 2006. Coherent spontaneous activity identifies a hippocampal-parietal memory network. J. Neurophysiol. 96, 3517–3531.

Vitz, P.C., 1964. Preferences for rates of information presented by sequences of tones. J. Exp. Psychol. 68, 176–183.

Vitz, P.C., 1966. Affect as a function of stimulus variation. J. Exp. Psychol. 71, 74–79.

Wagner, A.D., Shannon, B.J., Kahn, I., Buckner, R.L., 2005. Parietal lobe contributions to episodic memory retrieval. Trends Cogn. Sci. 9, 445–453.

Wallace, C.S., 2005. Statistical and Inductive Inference by Minimum Message Length. Springer, New York.

Wolpert, D.M., Goodbody, S.J., Husain, M., 1998. Maintaining internal representations: the role of the human superior parietal lobe. Nat. Neurosci. 1, 529–533.

Zhao, J., Al-Aidroos, N., Turk-Browne, N.B., 2013. Attention is spontaneously biased toward regularities. Psychol. Sci. 24, 667–677.